超軟弱粘性土 埋立地盤

渡 義 治（五洋建設(株)技術研究所 所長）

VERY SOFT RECLAMATION GROUND USING DREDGED COHESIVE SOIL

Y. WATARI

Engineering Research Institute
Penta-Ocean Construction Co., Ltd.

1. INTRODUCTION

With nearly 90% of the land consisting of mountainous terrain, Japan has been making efforts to build new land by reclaiming on shore areas through draining and filling in to expand the industrial and agricultural sphere for centuries. During the years between 1950 and 1960, many large scale reclamation projects were undertaken to build coastal industrial areas, and the reclamation technology using sea bottom material advanced markedly. However, the following geotechnical problems were not solved by the knowledge level available at that time, and they are still not fully solved today:

1) Fine particle soil is mixed with a large amount of sea water during the dredging process to form slurry, and this slurry is further diluted by sea water to increase the apparent volume in the process of dumping into the reclamation area. In the reclamation area, it gradually reduces its volume through sedimentation, deposition and self-weight consolidation, but comprehensive understanding of these processes is still lacking.

2) The clay, silt and other fine particle soil contained in the sea bottom soil deposit seaparates from the sand, gravel and other coarse grain soil to form an extremely soft layer, and the phenomenon of separate deposition is totally unclarified.

These two things have the key to solve the problems of determination the container volume of reclamation when decide the dredging soil volume at the sea bed. Then, this paper describe the investigation of sedimentation phenomenon at the reclamation area with cohesive soil obtained from the sea bottom by pump dredgers and one of the method to determine the sweetable reclamation container volume.

2. PHENOMENA WHEN DREDGED COHESIVE SOIL IS USED IN LAND RECLAMATION

2-1 General

When cohesive soil is dredged from the seabed by pump type dredger and dumped in the reclamation site, the soil particles are separated in the dredging pump and pipe and are conveyed to and dumped in the site.

At the reclamation site, the soil settles in the sea water and is deposited on the seabed. Although a large amount of sea water is

contained in the pores of the soil particles at the initial deposition stage, the volume commences to reduce simultaneously with deposition and advancement of self-weight consolidation. Sedimentation also commences with larger soil particles and separate deposition occurs.

This chapter describes the results of experiments and site surveys conducted in relation to these problems.

2-2 Sedimentation and Deposition

If sea water is added to cohesive soil obtained from the seabed and a sample with the same high water content as the deposit at the reclamation site is prepared and poured into a cylindrical container, and the sedimentation and deposition phenomena is observed one-dimensionally, it will take the course shown in Fig. 2-1 with the elapse of time.[1)]

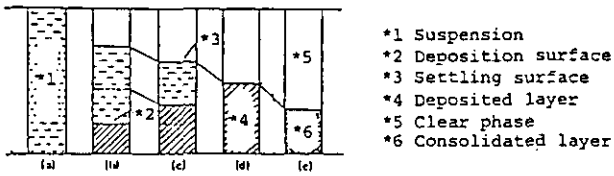

Fig. 2-1 Settlement and self-weight consolidation process

Sedimentation of the soil particles suspended in the water proceeds from state (a) at the start of the experiment with sedimentation beginning with the larger particles to form deposits at the bottom. The deposition layer gradually thickens as sedimentation of the suspended soil particles proceeds.

A clear phase forms at the upper layer of the muddy water with the lower layers being suspensions of increasing density. The boundary between these layers is called a sedimentation surface and suspension eventually disappears with the lowering of the sedimentation surface and rising of the deposition surface.

During this period, self-weight consolidation proceeds successively from the bottom of the deposition layer and decreases the volume, whereas new precipitation of soil particles increases the overall volume of the deposition layer. In actual reclamation sites, the state will be as (b) and (c) during the construction period, and will gradually change to state (d) when dumping of the dredged soil is completed.

2-3 One-dimensional Sedimentation and Deposition Experiment

If a one-dimensional sedimentation experiment is conducted using a graduated measuring cylinder and the settling state of the interfaces with passage of time is measured, the results will be as shown in Fig. 2-2. Consider the point at which the deposition layer rises and meets

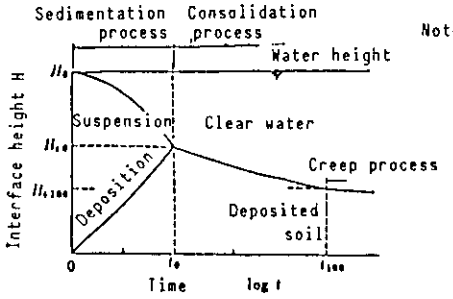

Note) *t_0 : Starting time of consolidation sedimentation
*t_{100} : Ending time of self-weigh consolidation
*H_{to} : Interface height when t_0
*Ht_{100}: Interface height when t_{100}

Fig. 2-2 State of sedimentation and consolidation process

the interface of the muddy water and clear phase as the starting time t_0 of consolidation sedimentation and the falling point of this sedimentation curve as the self-weight consolidation ending time t_{100}, and any further settling as the creeping process.

Set the height of the samples corresponding to each time as Ht_0 and Ht_{100}.

Next, show the sedimentation curve when the initial water content percentage W_i of the sample differs, as shown in Fig. 2-3.

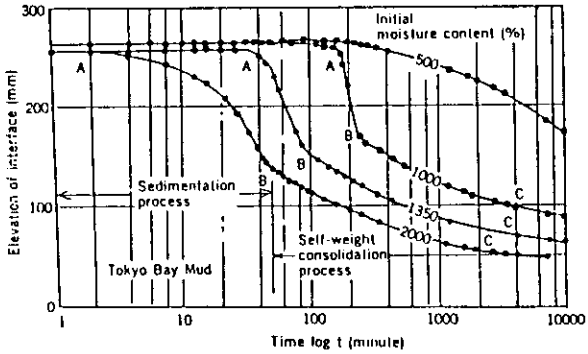

Fig. 2-3 Sedimentation curves plotted on log scale (Imai et al, 1976)

Although a clear sedimentation process cannot be observed when W_i is about 500%, the sedimentation and self-weight consolidation processes are distinctly observed when sending muddy water in slurry form, with a water content of over 1000%, to the reclamation site by a dredger. (In Fig. 2-3, A to B shows the sedimentation process and B to C shows the self-weight consolidation process.) This is because the soil particles mutually interfere and free sedimentation does not occur when W_i is only about 500%. Floculated free sedimentation occurs when W_i is over about 1000%.

Since the apparent volume of the dredged cohesive soil dumped in the reclamation site is expanded by mixing with sea water, the receiving capacity of the reclamation site must be sufficient to receive the dredged soil in expanded state. However, since the volume of the

deposited soil decreases with self-weight consolidation, large amounts of dredged soil can be dumped if the dumping time required to reach a fixed height is long or if the dumping time is short, since self-weight consolidation progresses more quickly. Fig. 2-4 shows the state when dredged soil was dumped in the reclamation area together with sea water on an experimental basis.

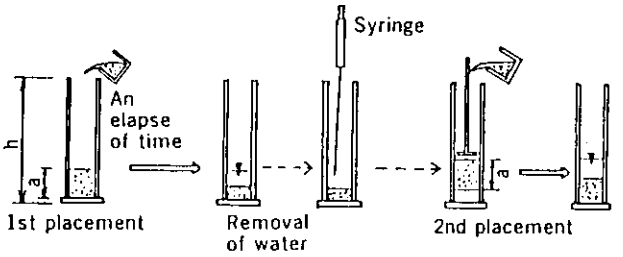

Fig. 2-4 Placing method of dredged soils (sedimentation test in laboratory)

Although upper layer sea water is discharged outside the reclamation area from the overflow at the site, in this experiment, muddy water was added while drawing out the upper layer water with a syringe. In this experiment, the pouring of dredged soil at the rate of 5 cm per hour is defined as a pouring speed of 5 cm/hr. Fig. 2-5 shows pouring of the dredged soil into the container at different speeds by setting the overall pour height of the dredged soil in suspended state to 100 cm and assuming the permissible pour height of the container (height of the embankment at the actual site) as 40 cm. Results of the experiment disclosed that the pour speed of the dredged soil under these conditions must be under 0.42 cm/hr or it will rise above the embankment at the site to flow outside the reclamation area.

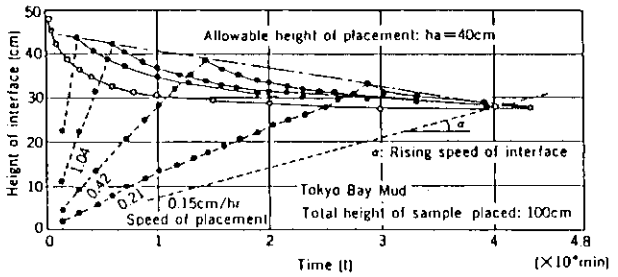

Fig. 2-5 Family of Sedimentation curves with different speeds of placement

In experiments using a graduated measuring cylinder of this type, cases may be considered in which the particle diameter of the upper and lower deposition layers will differ due to the large particle diameter soil settling first since the soil particles in the muddy water are not uniform and the problem of separate deposition arises. Sedimentation experiments are therefore being conducted using samples divided into a number of layers by causing precipitation in a large cylindrical container.

2-4 Two Dimensional Sedimentation and Deposition Test

The processes in the actual reclamation work are conceivably as follows:

1) The dredged soil is mixed with large amount of sea water in the suction mouth and the discharge pipe of the dredger to become completely dispersed, and at the outlet of the discharge pipe, it forms a slurry containing a large amount of soil particles and as much as 1,000% of water.

2) As this slurry is discharged into the reclamation area, it becomes further diluted by the sea water in the area, and the soil particles are brought to various parts of the area by the water flow.

3) The soil particles settle and deposit during this transportation process. Coarse particles deposit near the discharge pipe outlet, and finer particles are carried farther away by the flow from the discharge pipe outlet to result in separate deposition.

To verify this phenomenon by experiments, slurry specimens prepared with the same initial water content as the actual slurry were dumped in an experimental two-dimensional water tank simulating reclamation sites as specified in Table 2-1[2]. Fig. 2-6 shows the experimental equipment.

Table 2-1 Test condition

Case	Sample	W_0 (%)	d (mm)	q (ml/min)	U (m/sec)	H (min)	Pouring condition
S-I	Clay	1260	3	150	0.35	720	Continuous
S-II	Clay :6 + Sand :4	1000	4	120	0.16	720	"
L-I	Clay	1000	4	250	0.33	240	"
L-II	Clay	1000	6	500	0.29	150	"
L-III	Clay	1000	8	1000	0.33	120	"
L-IV	Clay :6 + Sand :4	1000	6	712	0.42	1320	"
L-V	Clay :6 + Sand :4	1000	6	700	0.42	1380	Separate

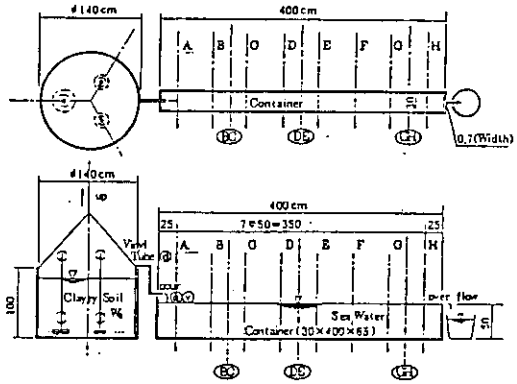

Fig. 2-6 Testing Apparatus

As muddy water was poured into the deposition tank, muddy water having a large specific gravity collects near the bottom of the tank in suspension. As the muddy water was continuously added, this soil suspension moved on the tank bottom in the form of a density current. (Photo 2-1)

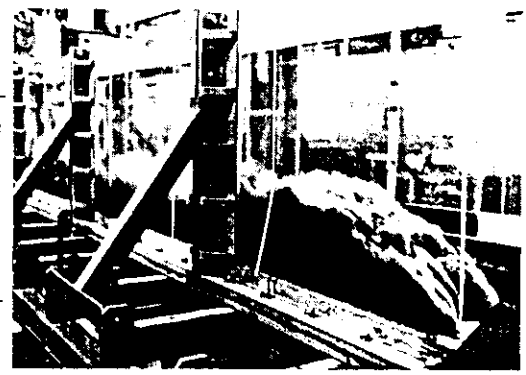

Photo 2-1 Moving state of suspension

Fig. 2-7 shows the water content distribution in the deposition tank for cohesive soil deposition, as measured with a water sam pler shown in Fig. 2-8. the measured water content was over 20,000% with the soil suspension, verifying the

existence of an extremely high water content phase.

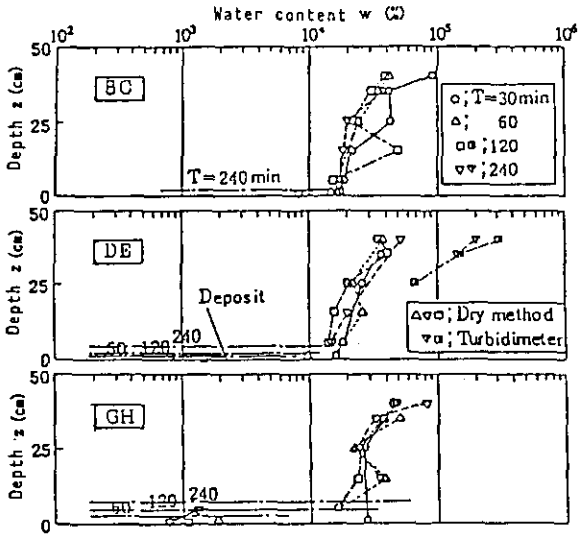

Fig. 2-7 Distribution of water content in deposition container

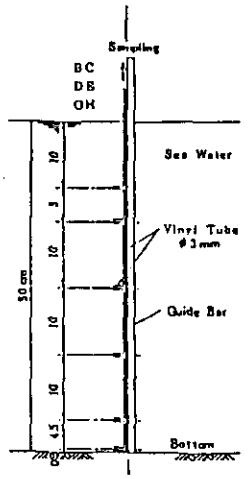

Fig. 2-8 Water and mud sampler

Photo 2-2 shows the sedimentation condition of deposit soil and soil particles. From this photo, the sedimentation mode of dredged soil can be thought of as a type of flocculated free settling.

Fig. 2-9 shows an example of the deposition state of cohesive soil, and Fig. 2-10 shows the process of increasing thickness of the cohesive soil layer, with the muddy water input volume plotted along the abscissa. In Fig. 2-10, the substantial influence of the muddy water input volume on the deposited soil thickness increase is shown.

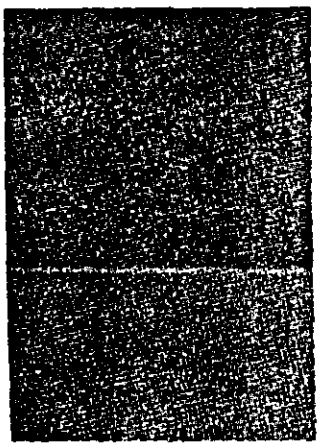

Photo 2-2 State of deposition and sedimentation of soil particles

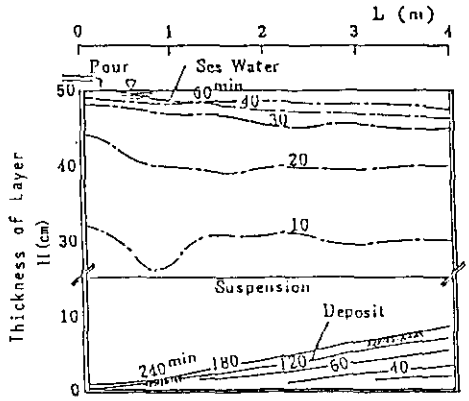

L − I

Fig. 2-9 Deposition state of cohesive soil

Next, when the same experiment was conducted using muddy water with sandy soil mixed in with cohesive soil, deposition resulted with the coarse particle soil completely separated. (Fig. 2-11, Photo 2-3)

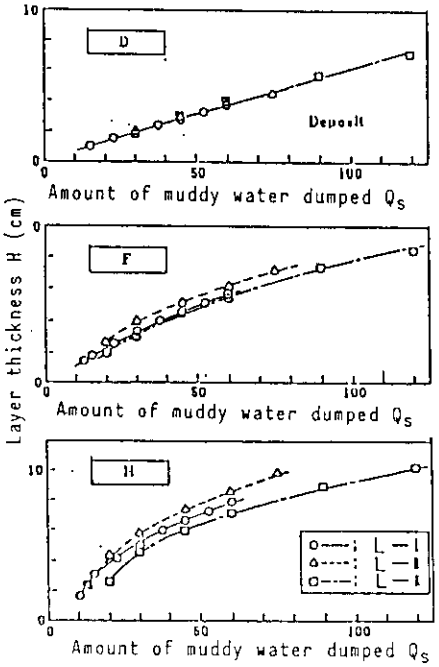

Fig. 2-10 Relation between amount dumped and thickness of deposited soil layer

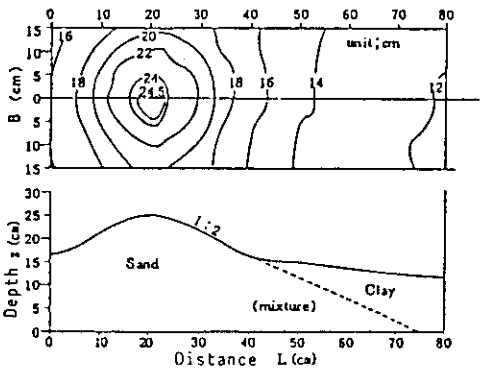

Fig. 2-11 Plane and cross sectional view of coarse particle deposits

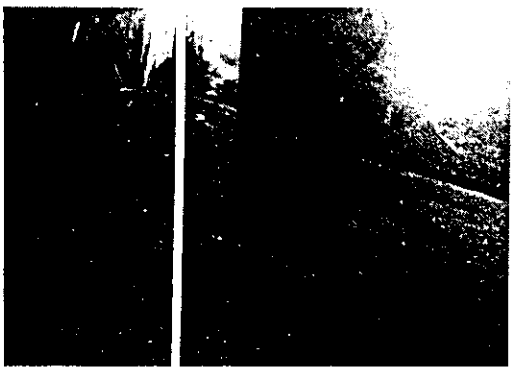

Photo 2-3 Deposition state of coarse grain soil

Soil tests were therefore conducted on deposition samples obtained at the point where muddy water was poured and at different distances from this point to obtain the soil characteristics of the deposited soil.

Fig. 2-12 and Fig. 2-13, respectively, show examples of the water content and grain size distribution. The water content has increased as the distance from the dumping point increased, and more finer grains are deposited as the distance increased, according to the grain size analysis results. Fig. 2-14 shows the grain size distribution according to the grain size division given in Table 2-5. Comparison between points D, F and H indicates no substantial difference in the contents of Sl_c, Sl_f and CL, but significant difference in COL contents.

Fig. 2-15 and Fig. 2-16 show the relationship between e and log p and consistency characteristics among various points. Clearly, the e ~ log p relationship and the consistency characteristics differ as the grain size of the deposited soil changes.

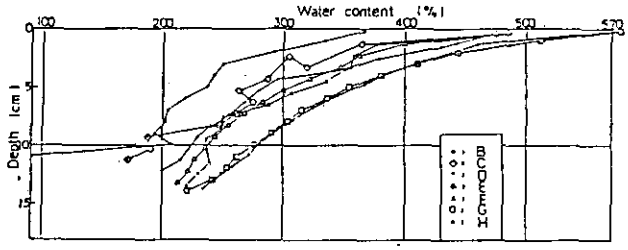

Fig. 2-12 Percentage of water content distribution diagram of deposit after self-weight consolidation

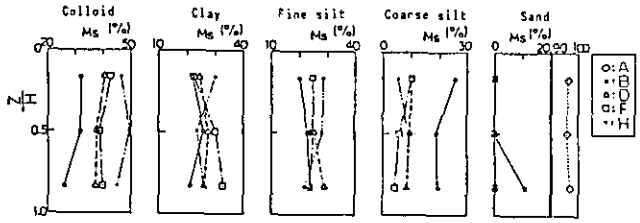

Fig. 2-14 Diagrams showing relation between Z/H and percentage of mass passed

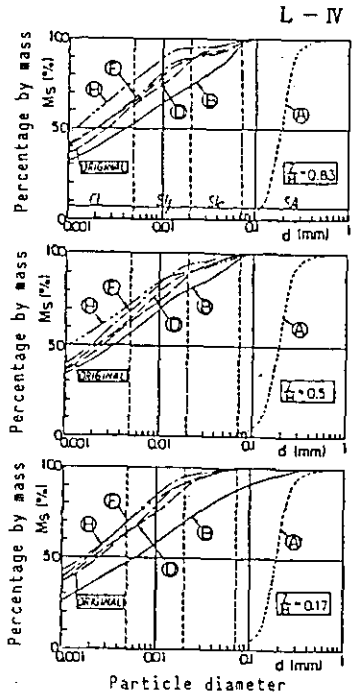

Fig. 2-13 Particle size curve of deposited soil

Table 2-2 Particle diameter classification

JIS	Colloid	Clay	Silt		Sand
	0.001	0.005		0.074	
Test	Colloid	Clay	Fine grain silt	Coarse grain silt	Sand
	0.001	0.005	0.02	0.074	

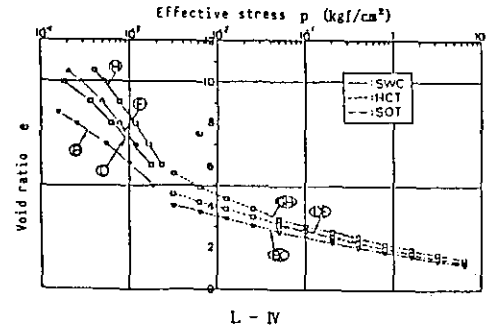

Fig. 2-15 e ~ log p curve

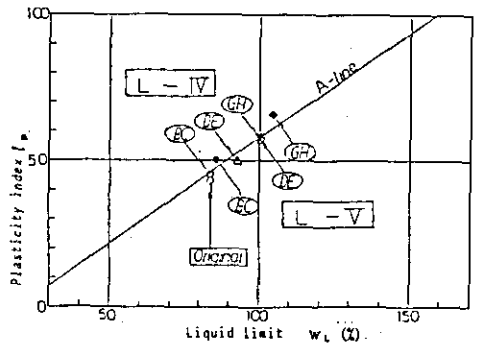

Fig. 2-16 Consistency characteristics

2-5 Site observation

Fig. 2-17 shows the deposition of cohesive soil as observed in the reclamation area during the reclamation work using dredged sea bottom cohesive soil in Kuhara District of Imari City, Japan. table 2-3 shows an outline of reclamation work specifications, Fig. 2-18 shows the plan view of the dredging and reclaiming areas, Table 2-4 shows the physical properties of the dredged soil, and Fig. 2-19 shows the dumping conditions of the dredged soil. From the start to the middle of the dredging period, the dumped soil deposited concentrically around the dumping point, but towards the end of the dredging period, the deposited soil thickness became nearly uniform throughout the reclamation area. This is interpreted as being caused by the settlement and deposition of the soil particles carried by the density current generated in the reclamation area up to the mid term of muddy water dumping, and as the overall movement of the deposited cohesive soil under the soil pressure towards the end of the period.

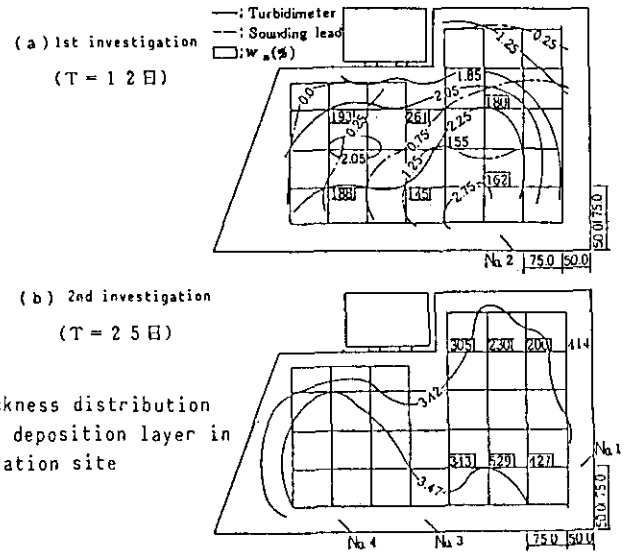

Fig. 2-17- Thickness distribution diagram of deposition layer in the reclamation site

Table 2-3 Reclamation outline

Kuhara district reclamation work	
Amount of soil dredged	467,200 m^3
Pump dredger horsepower	4,000 PS
Sand discharge pipe diameter	ϕ670 mm
Number of dredging days	31 Days
Area of reclamation site	272,000 m^2
Ground height before filling	-0.05 m
Top height of filling	+3.20 m

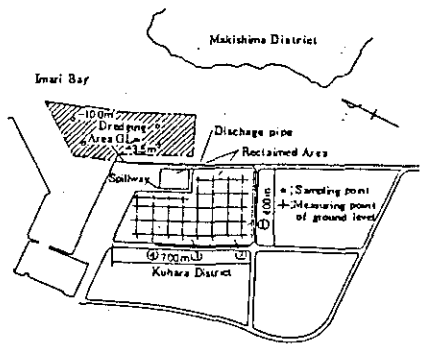

Fig. 2-18 Dredged reclamation plan

Table 2-4 Physical properties of Imari mud

	G_s	w_L	w_n	I_p	Clay	Silt	Sand
		(%)	(%)		(%)	(%)	(%)
Imari Bay Mud	2.62	92	95~100	64	40~47	48~52	5~8

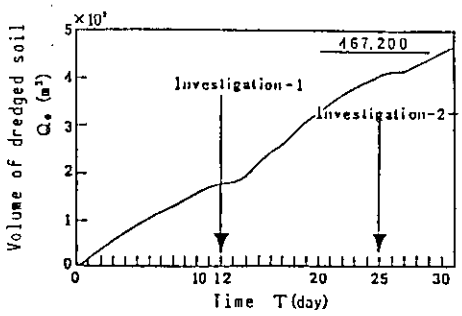

Fig. 2-19 Dumping state of dredged soil

In the reclamation site at Sakai-Senpoku harbor in Sakai City, Japan, soil properties were studied in the reclamation site at several points in one straight line starting from the dumping point, after the completion of the dredged soil dumping process. The dumping conditions of the dredged soil and the physical characteristics of the specimens are shown respectively in Fig. 2-20 and Table 2-5. Fig. 2-21 show the relationship between distance from the dumping point and sand contain volume. Sand was observed even at 300 meters away from the dumping point, but the sand content was seen to have decreased linearly with the distance up to 150 meters.

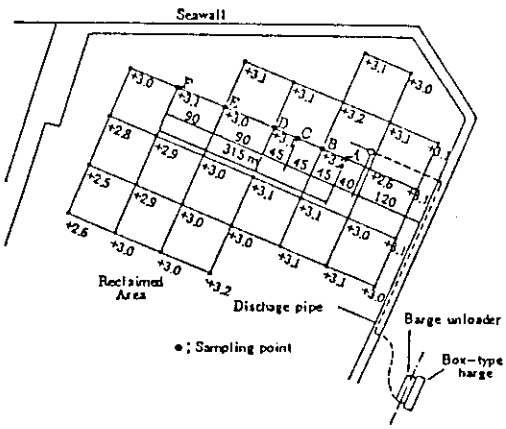

Fig. 2-20 Dumping state of dredged soil (SENBOKU)

Table 2-5 Physical properties of Yamato Estuary clay

	G_s	w_n	Clay	Silt	Sand
		%	%	%	%
Yamato Estuary Mud	2.62	80~150	38~50	44~60	2~8

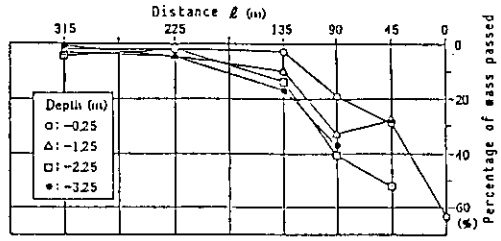

Fig. 2-21 Relation between distance and precentage of sand mass (Ms) passed

If the results of laboratory tests and the state at the site are compared, it may be considered that almost the same phenomenon is occurring according to survey results.

3. PREDICTION OF RECLAMATION LAND VOLUME BASED ON COHESIVE DEPOSIT SOIL SELF-WEIGHT CONSOLIDATION ANALYSIS

3-1 General

When soft cohesive soil of the sea bottom is dredged and dumped into reclamation sites, the cohesive soil settles and deposits to increase the thickness of the deposited soil layer with the progress of dredged soil dumping. However, the deposited soil layer also reduces its volume through progressive self-weight consolidation.

When planning dredging reclamation work based on the utilization of cohesive bottom soil, the depositing and self-weight consolidation behavior of cohesive soil must be taken into consideration in the procedure to be adopted.

Another important consideration in dredging reclamation plans is the predication of the reclamation land volume that permits the dumping of a specified volume of dredged soil, and a method of estimation based on self-weight consolidation analysis of deposited soil is described.

3-2 Analysis method

The possibility of theoretical analysis of the one-dimensional consolidation phenomenon of clay was first shown by Terzaghi. In his theory, Terzaghi assumed the deformation in the framed construction of clay was purely elastic.

By the consolidation analysis of the clay ground formed by dumped dredged soil at the reclamation work in Osaka Bay, Mikasa pointed out that in the consolidation analysis of ultra-soft clay layer, the following factors require study and proposed a consolidation equation incorporating these factors:[3)]

1) Influence of self-weight

2) Non-linearity of the stress-strain relationship and the stress-dependency of the permeability coefficient.

3) Changes in layer thickness.

Meanwhile, the analytical treatment of the soil consolidation processes became easy thanks to the recent remarkable development of computer technology and the adaptation method of the finite element method (FEM) of analysis. A one-dimensional consolidation analysis of cohesive soil was conducted on the basis of the FEM analysis of elastic consolidation as proposed by Sandhu, et al.[4)] and Yokoo, et al.[5)], with the above conditions taken into consideration.[6)]

a) Influence of self-weight

The initial water pressure h_{0i} at each node generated by the self-weight of soil can be easily obtained by the following formula:

$h_{0i} = \gamma_0' \cdot Z_i / \gamma_w$

where γ_0' = initial unit volume weight of clay in water

Z_i = depth from ground surface to i node

γ_w = unit volume weight of sea water

This h_{0i} is obtained prior to the consolidation calculation, and the analysis is made with the assumption that the initial excess water pressure h_{0i} is exerted within the soil.

b) Non-linearity of the stress-strain relationship and the stress-dependency of the permeability coefficient.

As the equation for the clay void ratio and effective stress relationship, the following is assumed:

(A) $e \sim \log p$ linear equation

$$e = e_1 + c_c \cdot \log p \tag{3.1}$$

(B) $\log e \sim \log p$ linear equation

$$\log e = a_1 + \beta \cdot \log p \tag{3.2}$$

Since the modulus of elasticity E is given by

$$E = (1 + e)dp/de,$$

E can be obtained with (3.1) and (3.2) as follows:

$$\text{(A)} \quad E = \frac{(1 + e_1 - c_c \cdot \log p) \cdot p}{\lambda} \tag{3.3}$$

$$\text{(B)} \quad E = \frac{[1 + \mathrm{Exp}(a_1 + \beta \cdot \log p)] \cdot p}{\mathrm{Exp}(a_1 + \beta \cdot \log p) \cdot \beta} \tag{3.4}$$

Expressions (3.3) and (3.4) indicate that as the effective stress of clay is continuously changed, the modulus of elasticity changes non-linearly. This means that the adoption of these expressions amounts to the adoption of the assumption that the relationship between effective clay stress and stress is non-linear.

On the other hand, with the elastic consolidation analysis by FEM, the E_i of each segmental element used in the consolidation calculation must be constant within the element. Denoting this constant E_i by $\overline{E_i}$, for the consolidation calculation based on the elastic consolidation analysis, incorporating the non-linearity of stress-strain relationship, we need to use the mean value of E_i that varies within each element.

An elastic consolidation calculation made with the given E_i and Δt yields displacement ΔU_{si} of this element as the difference between the displacements of nodes i and i + 1, and is expressed as follows:

$$\Delta U_{si} \ (= U_i - U_{i+1}) = \frac{\Delta Z_{0i} \cdot (\Delta_{pi} + \Delta_{pi} + 1)}{2 \cdot \overline{E}_i} \qquad (3.5)$$

On the other hand, from the viewpoint of the stress-strain non-linearity, displacement ΔU_{si} of this element accompanying the effective stress increase of the element is given by

$$\int_{z_i}^{z_2} \varepsilon \, dz$$

and by integrating this, we obtain the following:

(A) $$U_{hi} = \frac{\lambda \cdot \Delta Z_{0i}}{f_0} \cdot \left\{ \frac{P_{i+1} \cdot \ell_n(P_{i+1}) - P_i \cdot \ell_n(P_i)}{P_{i+1} - P_i} - 1 - \ell_n(P_0) \right\} \qquad (3.6)$$

(3.6)

(B) $$\Delta U_{hi} = \frac{\mathrm{Exp}(a_1/0.4343) \cdot \Delta Z_{0i}}{50} \cdot \left\{ P_0 - \frac{P_{i+1} - P_c}{(\beta + 1)(P_{i+1} - P_i)} \right\}$$

where $P_{i+1} = P_0 + \Delta P_{i+1}$,

$P_i = P_0 + \Delta P_i$,

P_0 = initial effective stress,

ΔP_i and ΔP_{i+1} = increment of effective stress produced by the decrease of pore water pressure between the two constituent nodes of element i,

Z_{0i} = initial layer thickness of element.

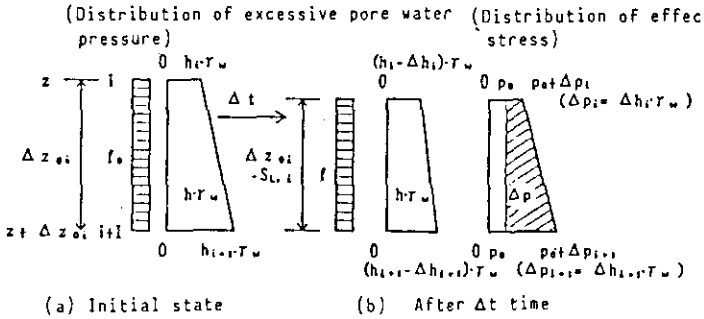

Fig. 3-1 Type diagrams showing state of excessive pore water pressure of element, and effective stress

In this case, ΔU_{si} and ΔU_{hi} must be equal. By making $\Delta U_{si} = \Delta U_{hi}$ in the FEM analysis, the non-linearity of the stress-strain relationship is incorporated in the analysis.

Furthermore, for the consolidation calculation, permeability coefficient k is needed, in addition to the modulus of elasticity. Generally, for the permeability coefficient, a linear relationship exists between log k and log p, and in our consolidation calculation, this linear relationship was used.

Assuming the relationship between ε and p to be expressed by (3.1) or (3.2), and k to be a function of effective stress p expressed by $k = f(p)$, we can find that k and E are paired one to one.

That is, when an assumed E is used to obtain p by Eq. (3.3) or (3.4), and the obtained p is substituted in $K = f(p)$, we can calculate k. Therefore, E and k were used in pairs in the consolidation calculation.

c) Change in layer thickness

In the present consolidation calculation, the strain corresponding to each increment Δt was calculated by the concept of micro-strain.

With this concept, displacement ΔU_1 during time Δt_1 after the initial state is given by the consolidation calculation using Δt_1.

Using displacement ΔU_1, we obtain the stress of this element by $\Delta \varepsilon_1 = \Delta U_1 / z_0$. However, since the layer thickness must change for subsequent time t_2, this effect must be compensated. The thickness of the element is assumed to be $z_1 - z_0 \ (1 - \Delta \varepsilon_1)$ in the consolidation calculation.

The strain during Δt_2 is calculated by $\Delta \varepsilon_2 = \Delta U_2 / z_1$, using the ΔU_2 obtained by the consolidation calculation. Therefore, although the strain during time Δt is calculated in micro-strain mode, the layer thickness corrected for the time prior to respective time increment Δt is used for the change of element layer thickness during the consolidation time period in the consolidation calculation.

Fig. 3-2 shows the flow chart for the consolidation analysis. Fig. 3-4 shows the result of the self-weight consolidation analysis conducted with the linear relationships between e and log p, and between log k and log p as shown in Fig. 3-3, under the one-side top drain condition at an initial layer thickness H_0 of 10 meters and an initial void ratio e_0 of 4. The result of the FEM calculation and the result of the finite difference method (FDM) based on Mikasa's consolidation theory are compared. The settlement curves were in good conformance between the two cases, with constant and increasing consolidation coefficient C_v.

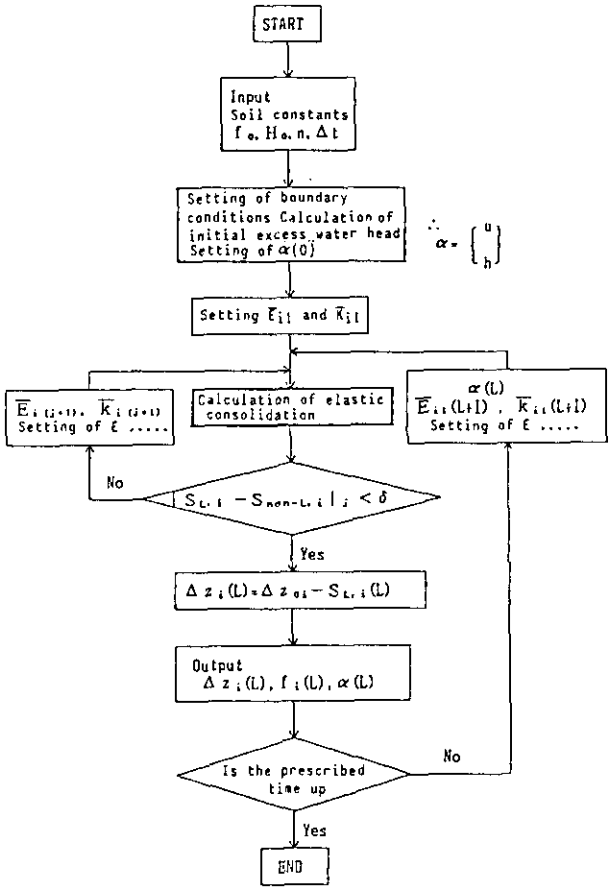

Fig. 3-2 Flow diagram of consolidation analysis

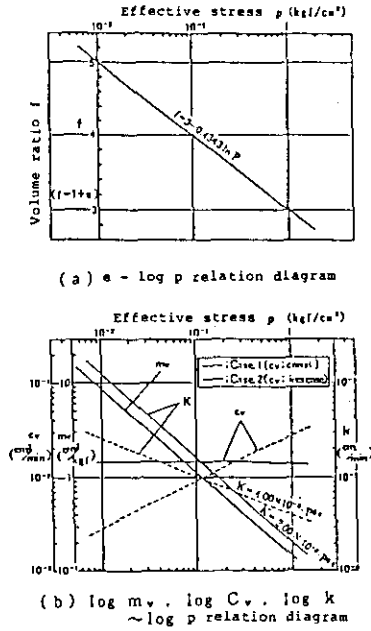

Fig. 3-3 Soil constants used in calculating consolidation

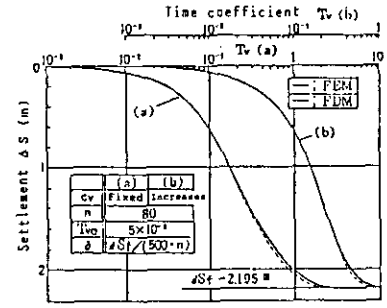

Fig. 3-4 Comparison of the settling curve of FEM and FDM

3-3 Indoor deposition experiment and its analysis

To analyze the self-weight consolidation of the deposited cohesive soil layer during the process of continuous deposition of dredged cohesive soil, the initial state of the deposited soil used in the analysis must be known, as the starting point of consolidation calculation.

As the method of determining the initial state, the concept of limit water content ratio as proposed by Mont et al. was used[7]. That is, the soil is considered to be formed and any effective soil stress is thought to be generated only when the precipitating cohesive soil reaches the bottom, and the void ratio as this initial state was denoted by e_i^*. When clay particles precipitate and deposit on the bottom to form soil with a void ratio of e_i^*, this e_i^* is used as the initial state data in the consolidation analysis calculation.

Then, e_i^* was obtained as follows:

1) Assuming the relationship between e and log p to be linear, a linear equation conforming fairly well with the consolidation test results was obtained.

2) In the initial state, e_i^* was assumed to be uniform, and the water content distributions after the compilation of the self-weight consolidation process for various e_i^* values were calculated.

3) Comparing the calculated and actually measured water content distributions after the completion of the self-weight consolidation, the e_i value that gave best conformance was taken as the value of e_i^*.

Fig. 3-5 shows the comparison of the calculated and actual water content ratio distributions.

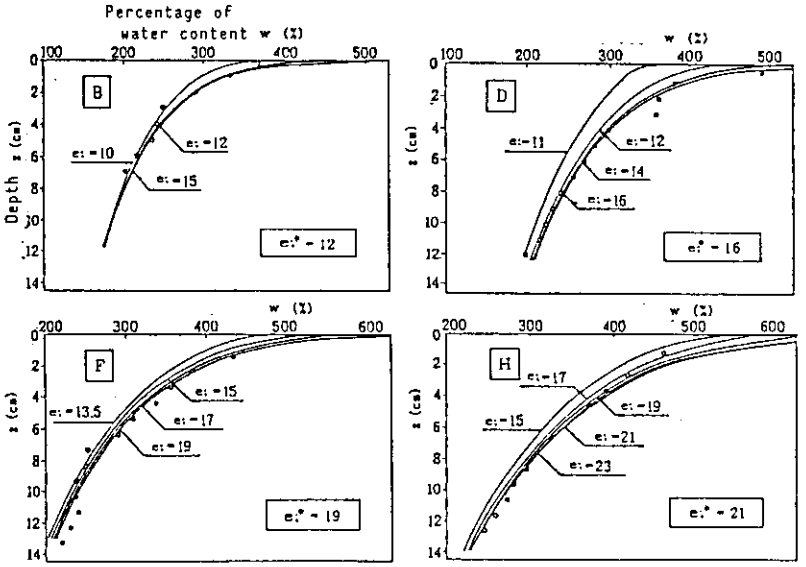

Fig. 3-5 Fitting state of percentage of water content distribution after self-weight consolidation is over

Because of the large deviation in the measured data, the conformity between the two is not good, but the value of e_i^* shown in the diagram was adopted.

Fig. 3-6 shows the e_i^* as determined in Fig. 3-5 on the straight line of e ~ log p equation.

As the e_i^*, the e value corresponding to $p = 10^{-5}$ kgf/cm^2 is considered to be appropriate.

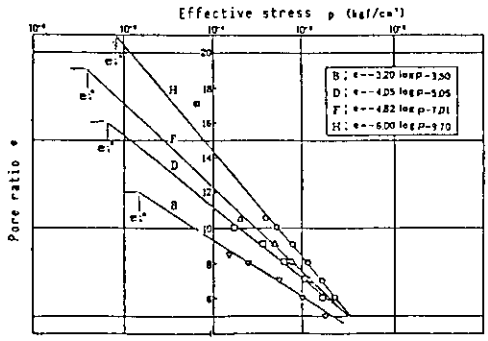

Fig. 3-6 e_i ~ log p relation diagram

To analyze the self-weight consolidation of cohesive soil during the continuous deposition process, the e ~ p relationship and the depositing speed of cohesive soil in the state of e_i* must be known, in addition to e_i*.

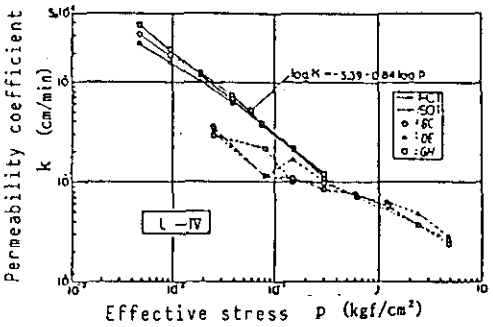

Fig. 3-7 k - p relation diagram

As the e ~ p relationship, the linear equations at various points in Fig. 3-6 were used, and as the k ~ p relationship, the relationship of Fig. 3-7 obtained from the indoor deposition experiment was used. The depositing speed (H_i*/t) of cohesive soil was calculated by the following formula:

$$H_i^*/t = \frac{\alpha \cdot Q_s}{A \cdot t} \cdot \frac{1 + e_i^*}{1 + e_s} \qquad (3.8)$$

where Q_s = muddy water dump volume at time t

A = cohesive soil depositing area

e_s = void ratio of dumped muddy water

α = volume ratio of cohesive soil in dumpted muddy water = 0.6

The compensation by α is important to eliminate the influence of separately deposited coarse grain soil.

Fig. 3-8 compares the increase of deposited soil layer thickness during the muddy water dumping process and the subsequent settling condition between the analysis data and the experimental values.

At point D, during the deposited layer increasing phase and during the subsequent settling phase, the measured data and the analysis data are fairly well in conformance.

On the other hand, at point H, considerable difference is seen between the two in the early deposited soil layer thickness increasing phase. The reason for this is that in a deposition experiment, the soil does not deposit in uniform thickness throughout the tank, differing from place to place, but in the analysis, the cohesive soil was assumed to deposit uniformly in solid volume in the experimental tank. This means that the difference was caused by the experimental method, and therefore, the analysis is considered to be applicable to the analysis of the actual reclamation work without undue error.

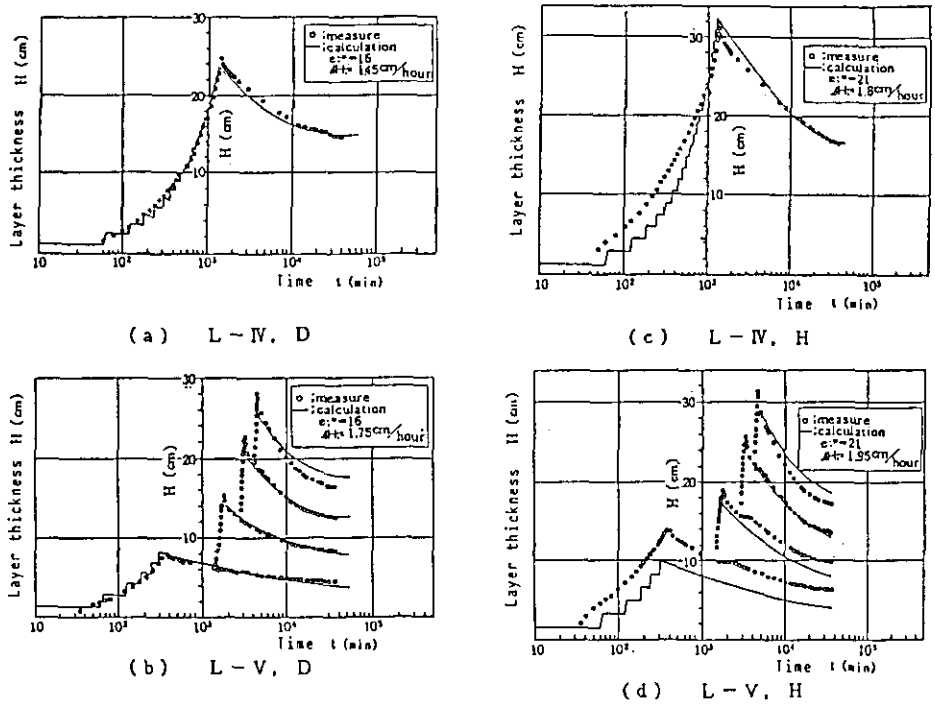

Fig. 3-8 Comparison of the process of increase in deposition layer thickness and settling by actual measurement and analysis

3-4 Analysis of actual reclamation work

At the dredge reclamation site in Hakozaki, Fukuoka Prefecture the depositing process of dredged soil was analyzed.

Table 3-1 shows the reclamation data, Fig. 3-9, reclamation site plan view, Fig. 3-10, the soil property study results, and Table 3-2 shows the physical properties of the specimens used in the consolidation characteristic study. Fig. 3-11 shows the consolidation characteristics.

Table 3-1 Outline of Hakozaki reclamation

Hakozaki reclamation work	
Amount of dredged soil	297,000 m^3
Pump dredger horsepower	2,250 PS
Sand discharge pipe diameter	φ660 mm
Dredging days	64 days
Area of reclamation site	72,000 m^2
Ground height before filling	-2.8 m
Top height of filling	+4.7 m

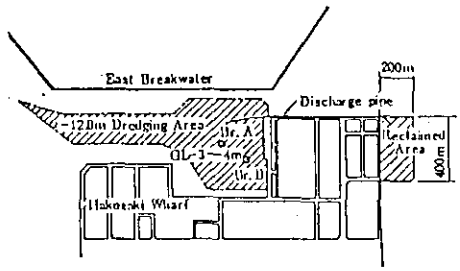

Fig. 3-9 Dredge reclamation plan (Hakozaki)

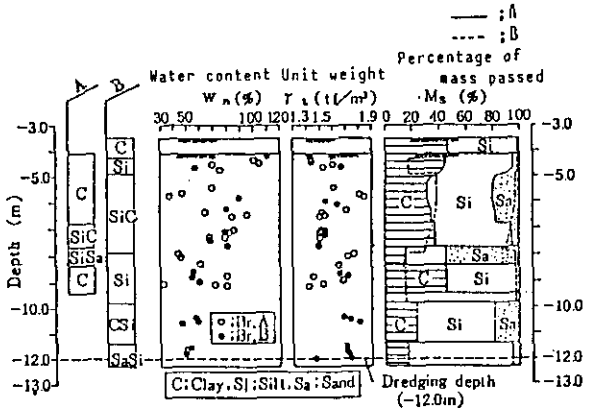

Table 3-2 Physical properties of the sample from which consolidation characteristics were obtained.

	G_s	w_L	I_p	Clay	Silt	Sand
Hakozaki Mud	2.69	78 (%)	49	41 (%)	53 (%)	6 (%)

Fig. 3-10 Soil investigation and test results

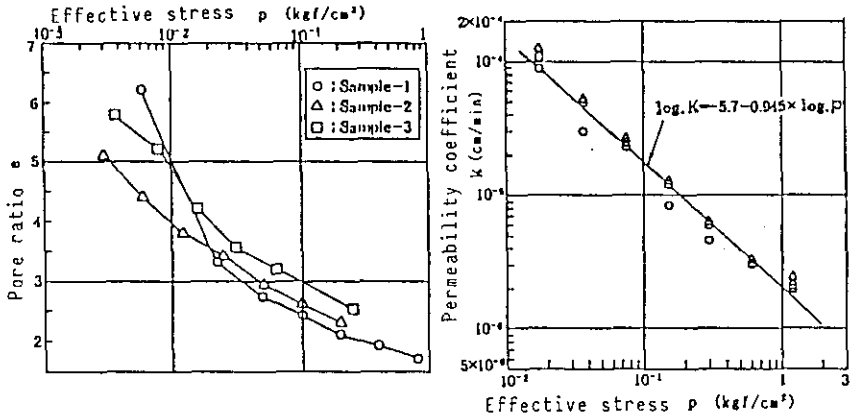

(a) Diagram of e - log p relations (b) Diagram of log k - log p relations

Fig. 3-11 Consolidation characteristics

The e ~ p relationship of the dredged cohesive soil tended to drop downward on the e ~ log p coordinate field (Fig. 3.11), but is considered to be approximately linear on a log e ~ log p coordinate plane (Fig. 3.12).

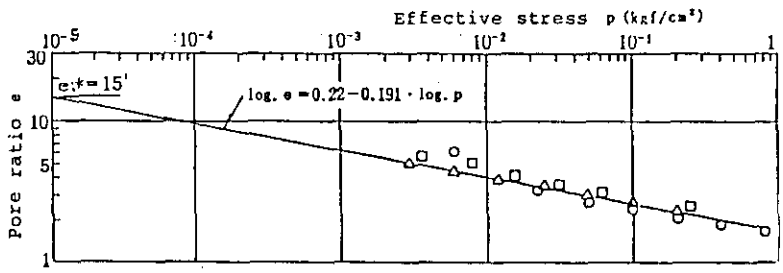

Fig. 3-12 Diagram of log e - log p relations (Hakozaki mud)

In the analysis of the dredged soil deposition process at Hakozaki, a linear equation of log e ~ log p was used. The e_i* value of 15 corresponding to p = 10^{-5} kgf/cm^2 was used.

The dredged soil dumping process for t = 33 days was represented by a continuous dumping curve shown by a dashed line in Fig. 3.13, and the dumping period t' was assigned to 0 to the 29th day and the days afterward were assigned to the still period.

The deposition speed of the dredged soil was calculated as follows:

$$H_i^*/t \approx \frac{1 + e_i^*}{1 + e_0} \cdot \frac{Q_0}{A \cdot t} \qquad (3.9)$$

where Q_0 = dredged soil volume in natural state at time t

A = area of reclamation land

e_0 = void ratio in natural state

In Fig. 3-13, the analysis result for H_i^*/t = 5.1 cm/day obtained in the above method is shown. A comparison between the analysis result and the actually measured deposited soil layer thickness increasing process (result of sounding lead measurement) showed a substantial difference. The cause for this was that a clay sample taken from the sea bottom was assumed to be a representative mean specimen of the dredged soil in the analysis. However, in the actual dredged soil, occasional substantial sand layers were contained, and such sandy soil resulted in a small volume in the deposited state, and had a very different consolidation characteristics.

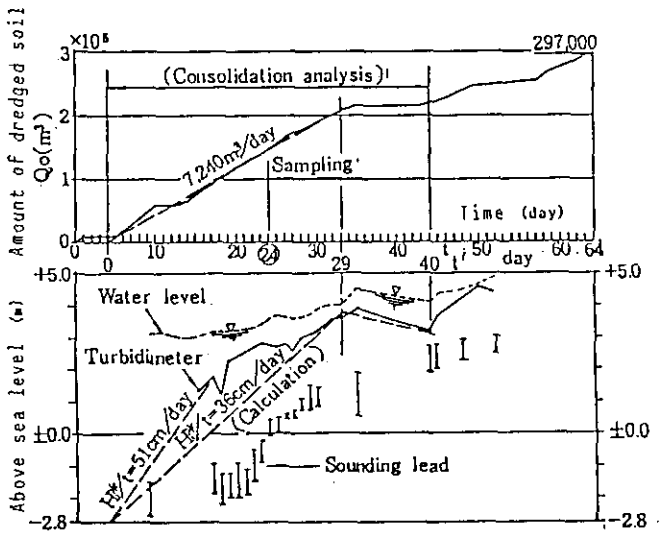

Fig. 3-13 Investigation results of dumping state of dredged soil and height of deposition layer

To make the analyzed deposited soil layer thickness increase speed conform to the actually measured one, the value of α in $H_i^*/t = \alpha \cdot H_i^*/t$ ($\alpha < 1$) was changed and recalculated. Fig. 3-13 shows the result obtained with $\alpha = 0.7$, giving $H_i^*/t = 36$ cm/day. With this result, the actual and the analyzed soil deposition slope more approximately conformed.

3-5 Preparation of deposition pre-estimation diagram

By changing H_i^*/t diversely, the deposition process of continuously dumped dredged soil was calculated with the linear equations of log e ~ log p and log k ~ log p, using $e_i^* = 15$, and the deposition preestimation diagram of Fig. 3-14 was obtained. With Fig. 3-14, the following predictions are possible:

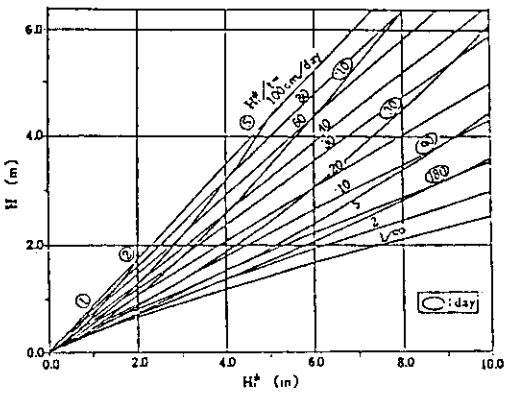

Fig. 3-14 Diagram showing the relation between dredged soil height H_i calculated in state e_i, dumping speed H_i/t and height H of the deposited soil

1) From the total soil volume (V_0) and the mean void ratio (e_0) of the dredged soil in the natural state on the sea bottom before the dredging, the total dumped height H_i^* in the reclamation area for e_i^* is calculated as follows:

$$H_i^* = \frac{1 + e_i^*}{1 + e_0} \cdot \frac{V_0}{A} \qquad (3.10)$$

2) The dumping speed required to dump the dredged soil with H_i^* into the reclamation area having a height of H is the value of H_i^*/t for H and H_i^*.

When the point corresponding to H and H_i^* is located on the lower right side of the line of $H_i^*/t = 1/\infty$, the dredged soil having H_i^* cannot be dumped into this reclamation area.

3) When H, A and H_i^*/t are given, the dredged soil volume V_0 that can be dumped into the reclamation area can be obtained by substituting the H_i^* that corresponds to the given H and H_i^*/t into the above equation.

When the consolidation characteristics of the actual soil at the site are known from specimen soil sampled at the site, and a deposition pre-estimation diagram is worked out, the relationship between the dredging soil volume and the dumping volume into the reclamation area can be clearly determined.

4. CONCLUSION

The principal conclusions reached as a result of the experiments and site investigations are as follows.

1) Sedimentation of dredged cohesive soil becomes floculated free sedimentation.

2) Cohesive soil deposition at the site will be conducted concentrically, centered on the slurry dumping point, since the water currents generated in the reclamation site will carry away the cohesive soil during the initial and intermediate dumping period. In the later period however, the deposition layer thickness becomes uniform with fluid sideward movements of the deposited soil.

3) Coarse and fine soil particles will be deposited in completely separate state. The coarse soil particles are deposited near the dumping point whereas the fine soil particles will be carried by the current and deposited further away. The cohesive soil is also separated and deposited and the soil characteristics differ depending on the distance from the dumping point of the muddy water.

4) Self-weight consolidation analysis of the continuous deposition process of dredged cohesive soil is possible by the F.E.M. analysis method.

5) The value e corresponding to $p = 10^{-5}$ kgf/cm^2 may be considered as the criterion for e_i^* corresponding to the limit water content ratio for use in analysis of the continuous deposition process of cohesive soils.

6) The thickening process of the deposition layer during the continuous dumping period of dredged cohesive soil varies greatly with dumping speed H_i^*/t. In setting up dredging plans, it will therefore be effective to use diagrams showing dredged soil height H_i^* and H_i^*/t converted to e_i^* state, and height H of the deposition.

After completing the reclamation work in the foregoing manner, dehydration occurs on the surface of the deposited layer from solar drying together with advancement in self-weight consolidation, thus realizing bearing the capacity of the soil.

A partial explanation of sedimentation and deposition of soil particles in reclamation work was given in this paper and we hope that this will serve as reference for our readers.

REFERENCE

1) Yano, I.; Imai, G.; Tsuruya, K.: Settlement and self-weight consolidation of soil dredged by pump dredger, Penta-Ocean Construction Co., Ltd. Annual Technical Review, 1976, pp 1 ~ 5, 1977 (in Japanese)

2) Watari, Y.; Shinsha, H.; Hayashi, K.; Aboshi, H.: Settlement and separate deposition of dredged cohesive soil; Research report of Engineering Dept., Hiroshima University, Vol. 34 No. 2, pp 175 ~ 187, 1986 (in Japanese)

3) Mikasa, M.: Consolidation of soft clay, Kajima Publishing, 1963 (in Japanese)

4) Sandhu, R.S.; and Pister, K.S.: Variational Principles for boundary value and initial-boundary value problems in continuum mechanics, Int. Journ. Solid-Structure, Vol. 17, pp 639 ~ 654, 1971.

5) Yokoo, Y.; Yamagata, K.; and Naraoka, H.: Finite element method applied to Biot's consolidation theory, Soils and Foundations, Vol. 11 No. 1, pp 29 ~ 46, 1971.

6) Watari, Y.; Shinsha, H.; Hayashi, K.; Aboshi, H.: Dredge soil volume pre-estimation based on self-weight consolidation analysis of cohesive reclamation soil, Research report of Engineering Dept., Hiroshima Univ., Vol. 34, No. 2, pp 159 ~ 173, 1986 (in Japanese)

7) Monte, J.L.; and Krizek, R.J.: One-dimensional mathematical model for large-strain consolidation, geotechniques, Vol. 26, No. 3 pp 495 ~ 510, 1976.